2015-01-0834
Published 04/14/2015

doi:10.4271/2015-01-0834
saeeng.saejournals.org

# GDCI Multi-Cylinder Engine for High Fuel Efficiency and Low Emissions

Mark Sellnau, Wayne Moore, James Sinnamon, Kevin Hoyer, Matthew Foster, and Harry Husted
Delphi Powertrain

## ABSTRACT

A 1.8L Gasoline Direct Injection Compression Ignition (GDCI) engine was tested over a wide range of engine speeds and loads using RON91 gasoline. The engine was operated with a new partially premixed combustion process without combustion mode switching. Injection parameters were used to control mixture stratification and combustion phasing using a multiple-late injection strategy with GDi-like injection pressures.

At idle and low loads, rebreathing of hot exhaust gases provided stable compression ignition with very low engine-out NOx and PM emissions. Rebreathing enabled reduced boost pressure, while increasing exhaust temperatures greatly. Hydrocarbon and carbon monoxide emissions after the oxidation catalyst were very low. Brake specific fuel consumption (BSFC) of 267 g/kWh was measured at the 2000 rpm-2bar BMEP global test point.

At medium load to maximum torque, rebreathing was not used and cooled EGR enabled low-temperature combustion with very low NOx and PM, while meeting combustion noise targets. MAP was reduced to minimize boost parasitics. Minimum BSFC was measured at 213 g/kWh at 1800 rpm - 12 bar IMEP.

Full load torque characteristics of the engine were developed using alternative injection strategies. Maximum BMEP of 20.3 bar was measured at 2000 rpm, with 17.4 bar BMEP achieved at 1500 rpm. Torque objectives for this engine were met. Transient co-simulations demonstrated the potential for good combustion control during hard accelerations and gear shift transients.

**CITATION:** Sellnau, M., Moore, W., Sinnamon, J., Hoyer, K. et al., "GDCI Multi-Cylinder Engine for High Fuel Efficiency and Low Emissions," *SAE Int. J. Engines* 8(2):2015, doi:10.4271/2015-01-0834.

## INTRODUCTION

Throughout the world, many efforts are being made to improve the thermal efficiency of automotive internal combustion engines. One relatively new approach is gasoline partially-premixed compression ignition (PPCI) that was introduced by Kalghatgi [1] and first tested by Johansson [2]. Widespread interest in PPCI has led to numerous studies, which have contributed to a significant body of PPCI test data and experience. Tests have been performed on diesel engines using various gasoline-like fuels at Shell [3, 4, 5, 6], Lund [7, 8, 9, 10], Cambridge [11], UW-Madison [12, 13, 14, 15, 16], Argonne [17, 18, 19, 20], Tsinghua [21], and RWTH [22]. In practically all cases, diesel-like efficiency was measured.

Various injector designs and piston designs have also been developed with significant improvements. Delphi [23, 24, 25, 26, 27] reported single-cylinder and multi-cylinder engine test results with various injectors using single, double, and triple injection strategies.

Engine tests have also been performed using naphtha fuels [28, 29]. Naphtha has significantly lower octane number (RON 70 to 84) and processing cost compared to current market gasoline. This work has shown compatibility of the PPCI combustion process with lower octane fuels in a longer term perspective.

As part of a US Department of Energy funded program, Delphi has been developing a multi-cylinder engine concept for PPCI combustion with current US market gasoline (RON91)[30]. Delphi uses the term Gasoline Direct Injection Compression Ignition in reference to this combustion process. A description of the first-generation 1.8L four-cylinder GDCI engine, including injection, valvetrain, boost, and exhaust subsystems was reported [30]. The engine was operated “full time” [25] over the operating map with partially premixed compression ignition. No combustion mode switching, diffusion controlled combustion, or spark plugs were used. The engine was packaged in a D-class passenger vehicle.

One program objective was to achieve diesel-like fuel efficiency with engine-out NOx and PM emissions below that needed for NOx or PM aftertreatment. Combustion noise levels (CNL) and combustion stability (COV IMEP) were constraint factors. Other program

objectives included demonstration of good transient load response and room temperature cold starts. Preliminary targets for engine development and testing are shown in Table 1.

Table 1. Preliminary Targets for Engine Testing.

| | |
|---|---|
| Engine Out NOx | ≤ 0.2 g/kWh |
| Engine Out PM | ≤ 0.1 FSN |
| CNL | load dependent |
| COV IMEP | ≤ 3% |
| Combustion Efficiency | ≥ 95% |

In the current work, the first generation 1.8L GDCI engine was tested over a range of steady-state operating conditions using the latest GDCI injection system. For low loads, an exhaust rebreathing strategy was evaluated. Calibration mapping was conducted over a wide range of operating conditions used on the FTP drive cycle. Preliminary full load testing was performed to develop full load torque characteristics of the engine. Finally, aggressive gear shift transients were simulated with high rate of load change.

## GDCI CONCEPT AND INJECTION STRATEGY

The GDCI engine concept combines the best of diesel and spark-ignited engine technology. Like diesel engines, the compression ratio is high, there is no intake throttling, and the mixture is lean for improved ratio of specific heats. GDCI uses a new low-temperature combustion process for partially-premixed compression-ignition. Multiple-late-injections of gasoline (RON91) vaporize and mix very quickly at low injection pressure typical of direct injected gasoline engines. Low combustion temperatures combined with low mixture motion and reduced chamber surface area significantly reduced heat losses.

A schematic of the GDCI combustion chamber concept is shown in Figure 1. The engine features a shallow pent roof combustion chamber, central-mounted injector, and 15:1 compression ratio. A quiescent, open chamber design was chosen to support injection-controlled mixture stratification. Swirl, tumble, and squish were minimized since excessive mixture motion may destroy mixture stratification created during the injection process. The piston and bowl shape were matched with the injection system and spray characteristics. The bowl is a symmetrical shape and was centered on the cylinder and injector axes.

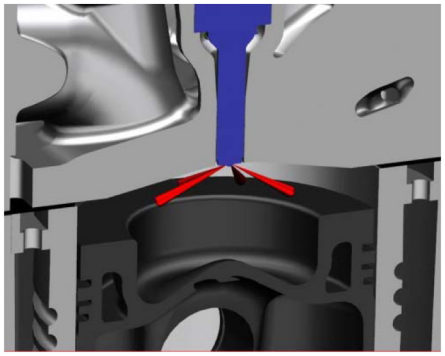

Figure 1. GDCI Combustion Chamber Concept.

The GDCI injection strategy is central to the overall GDCI concept and is depicted in the Phi-T (equivalence ratio-temperature) diagram shown in Figure 2. The color contours in Figure 2 show simulated CO emissions concentration. The injection process involves one, two, or three injections during the compression stroke, which are shown as quantities Q1, Q2, and Q3. Each injection begins in the upper left of the Phi- T diagram (liquid) and quickly vaporizes and mixes to Phi less than 2 by the start of combustion (SOC). At SOC the fuel-air mixture is stratified to achieve stable ignition and controlled heat release. Wall wetting is minimized and fuel is kept away from cold zones such as the piston topland and cylinder liner that may impede complete oxidation.

The ideal "stratification line" is shown in Figure 2 and represents the ideal injection process. To achieve low NOx and low PM emissions simultaneously, combustion must occur "in the box" shown in Figure 2 (avoiding soot and NOx formation regions). To also minimize CO emissions, which can compromise efficiency, combustion must occur in the smaller region defined by 0<Phi<1.2 with 1300<T<2200 degrees K. Therefore at SOC, which is approximately top-dead-center (TDC), all parcels in the combustion chamber should be no richer than Phi of approximately 1.2. This corresponds to the top of the stratification line in Figure 2. The stratification line is inclined due to charge cooling effects with the richest parcels cooling more than the leanest parcels. Extensive KIVA simulations with this combustion system and an injector spray model were reported in 2014 [30].

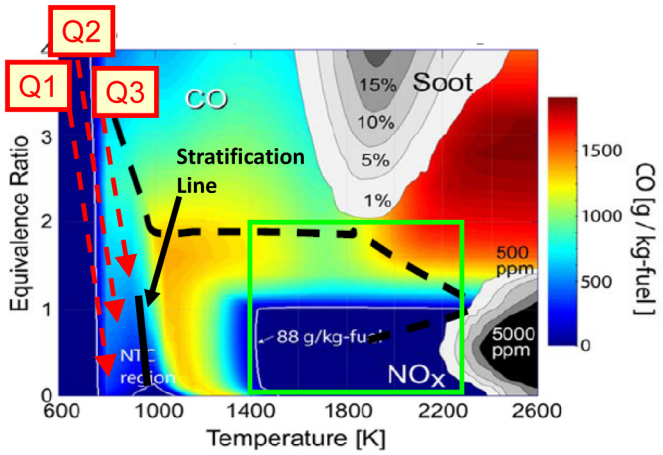


Figure 2. GDCI Injection Strategy depicted on Phi-T Diagram with NOx, Soot, and CO Contours.

## ENGINE DESCRIPTION

Base engine specifications for the GDCI engine are listed in Table 2. The engine has 1.8L displacement, four-cylinders, and four-valves-per-cylinder. Bore, stroke, and connecting rod length are 82 mm, 85.2 mm, and 144.7 mm, respectively, for B/S of 0.96 and r/l of 0.29. With geometric compression ratio of 15, this engine has geometry similar to modern light duty diesel engines. A photograph of the first assembled GDCI engine is shown in Figure 3.

Table 2. Base Engine Specifications.

| | |
|---|---|
| Engine Type | GDCI |
| Configuration | In Line 4-Cylinder |
| Displacement | 1.8 L |
| Bore-Stroke-Rod | 82 x 85.2 x 144.7 mm |
| Piston Pin Offset | 0.5 mm |
| Compression Ratio | ~15 |
| Chamber | Shallow Pent Roof |
| Peak Cyl. Pressure | 200 bar |
| Injection | Central-Mount GDI |
| Valvetrain | 4V DOHC Type II |
| Piston | GDCI Design |
| Swirl | none |

Figure 3. GDCI 1.8L Multi-cylinder Engine.

Cylinder Head The cylinder head is an all new design with four-valves-per-cylinder rated at 200 bar peak cylinder pressure (PCP) for development purposes. The injector is central-mounted without offset or inclination relative to the cylinder axis. The combustion chamber features a shallow pent roof with valves flush with the pent roof surface. Intake and exhaust ports were developed for good flow characteristics but without the need for swirl, tumble, or squish. A double overhead camshaft, Type II valvetrain with roller finger followers and rollerized camshafts was selected due to low friction and compact packaging. Automotive grade cylinder pressure sensors were used for combustion control and were mounted under the intake ports with near flush mounting. In addition, Kistler cylinder pressure transducers were mounted vertically at the cylinder periphery. No spark plug exists in the cylinder head. Overall, the cylinder head is very compact and employs conventional aluminum casting methods and alloys, while meeting demanding structural requirements.

Piston A new piston was designed for GDCI based on extensive KIVA simulations. The piston bowl shape and injector spray characteristics were matched for typical GDCI injection timings. This resulted in significantly reduced piston surface area and less propensity for wall wetting relative to typical diesel pistons. The piston bowl is symmetrical and is located on the cylinder axis [27].

Injection System Previous work by the authors has demonstrated improved GDCI combustion performance through injection system developments [23, 24, 25, 26, 27,30]. Simulation tools were used to develop injector spray characteristics that provide very fast vaporization and low spray penetration, while also providing the necessary injection rate (flow rate). Designed experiments on a single-cylinder engine were used to determine best injection timings, quantities, and injection pressures for various injector designs. Injection pressures were in line with current trends for GDi engines. In general, low injection pressures are desirable to reduce pump parasitics and fuel system cost.

The GDi fuel pump was mounted at the end of the cylinder head and was driven by the exhaust camshaft. The pump shaft has four lobes and exhibits excellent rail pressure control via modulation of the spill valve. The fuel rail has inlet and outlet orifices for dampening of pressure pulsations in the system. Injector drive waveforms were developed to support the multiple late injection strategies used for GDCI. Importantly, the system delivers accurate fuel quantities for multiple injections in all cylinders.

Valvetrain System Full-time GDCI combustion over the operating map is achievable by using exhaust rebreathing (RB) at low loads and cooled EGR at medium to higher loads. Rebreathing (RB) is accomplished using the exhaust valvetrain system, which provides a secondary exhaust lift event during the intake stroke. A Delphi electric camshaft phaser is used to actuate the exhaust valvetrain and control the secondary valve lift with very fast response. It is an effective method to recuperate heat from hot exhaust gases in order to raise mixture temperatures. This heat promotes autoignition at low loads when boost pressure is zero or low. Rebreathing also collapses the pumping loop (intake and exhaust valves are open at same time) and raises exhaust temperatures significantly. In this way, a close-coupled oxidation catalyst will remain active over a wide range of low loads without special maintenance heating.

Boost System Intake boosting is difficult for low-temperature engines because the exhaust enthalpy to drive a turbocharger is very low. Extensive engine simulations were performed [26] to develop a boost system that provides the necessary intake boost with low boost parasitics. The system includes a variable geometry turbocharger, a supercharger with clutch, and two charge coolers. Figure 4 shows a schematic of the boost system. No intake throttle is used.

The low pressure loop exhaust gas recirculation (LPL-EGR) system is also shown in Figure 4. The exhaust gases exit the turbine and pass through a close-coupled oxidation catalyst to reduce HC and CO emissions. The EGR system is designed for high flow in a compact layout for fast response on the vehicle.

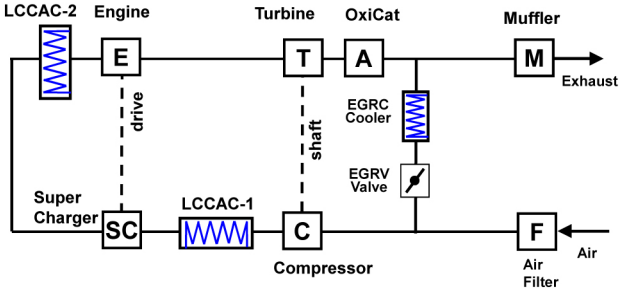


Figure 4. Schematic of boost system with charge air coolers and LPL-EGR.

Exhaust System and Aftertreatment Figure 5 shows a photograph of the exhaust system used on the first generation (Gen I) multi-cylinder GDCI engines. The aftertreatment system is comprised of only an oxidation catalyst. The intent is to satisfy tailpipe NOx and PM emissions targets using clean GDCI combustion technology without NOx or PM aftertreatment. The oxidation catalyst is close-coupled to the turbocharger outlet for heat conservation. The entire exhaust system including flex pipes and sensors is packaged for the GDCI vehicle application. An exhaust pipe and muffler were used for dynamometer testing to emulate the restriction of the vehicle exhaust system.

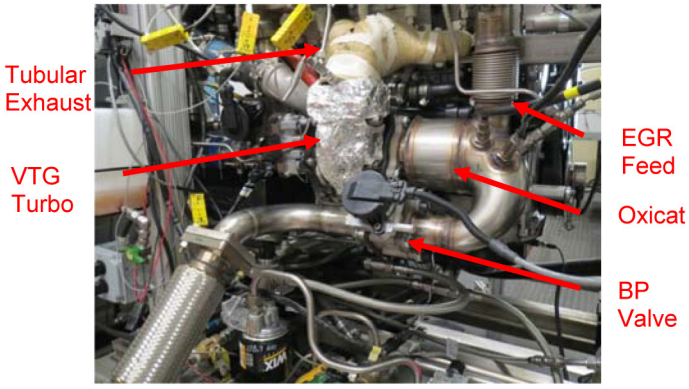


Figure 5. Photograph of GDCI exhaust system on a dynamometer engine.

## EXPERIMENTAL METHODS

Experiments were performed on an engine dynamometer at Delphi. The test fuel was Shell regular unleaded gasoline with approximately 10 percent ethanol and research octane number (RON) of 91, as is representative of commercial gasoline fuel in the United States. Fuel property data are listed in Table 3.

Table 3. Properties of Shell Test Fuel.

| Parameter | Units | E10 |
|---|---|---|
| Density | g/cc | 0.7402 |
| H/C Ratio | atomic | 2.062 |
| O/C Ratio | atomic | 0.0349 |
| LHV | MJ/kg | 42.03 |
| Octane | | 87.6 |
| RON | | 91.7 |
| MON | | 83.4 |
| T0 | C | 40.4 |
| T50 | C | 102.4 |
| T100 | C | 217.9 |
| Aromatics | vol% | 18.7 |
| Olefins | vol% | 11.2 |
| Saturates | vol% | 70.1 |
| Ethanol | vol% | 9 |
| Sulfur | ppm | 27.8 |

Engine air flow was measured by a Meriam laminar flow element with a 55 gallon surge tank located upstream of the engine. Combustion air was conditioned for temperature and humidity. Fuel flow was measured with an AVL 735 Fuel Mass Flow Meter in combination with an AVL 753 Fuel Temperature Controller. Fuel flow data for operation on E10 fuel was corrected to E00 based on the lower heating value of the test fuel.

Exhaust emissions were measured conventionally. Non- dispersive infrared analysers were used for CO2, CO, and intake CO2 species. Intake $CO_2$ data was used to calculate EGR levels. A chemiluminescence analyser was used for NOx species, a heated flame-ionization detector was used for total HC, and a paramagnetic analyser was used for O2. Exhaust smoke was measured with an AVL 415S smoke meter. Exhaust particulate size distribution was measured with a TSI 3090 Engine Exhaust Particle Size Spectrometer [31, 32]. The sampling system for exhaust particulate is described in [24].

Cylinder pressure was measured with a flush-mounted Kistler 6125CU20 pressure transducer. These transducers were inserted from the top of the cylinder head and located flush with the chamber near the cylinder bore. A Kistler 2614 crankshaft encoder provided crank position data and was dynamically aligned with engine TDC using a Kistler 2629B TDC probe. Cylinder pressure data was sampled every 0.5 CAD. Indicated mean effective pressure (IMEP) was reported on a gross basis. Combustion noise level (CNL) was measured using an AVL FLEXIFEM Noise Meter [33].

Lab Engine Controller The engine controller is based on National Instruments hardware and LabView software [34], and was built by National Instruments-San Antonio. The system schematic is shown in Figure 6. The controller features realtime combustion analysis using NI Combustion Analysis System (NI-CAS) and allows rapid prototyping of test cell engine control software using LabView. The controller is comprised of a National Instruments 8110 Real-Time processor, two PXi 7813R 3M gate field programmable gate arrays (FPGA), two PXi 6123 modules for fast data acquisition, a PXi 8512 for CAN communications, and numerous cRIO modules for interfacing to engine sensors, actuators, and other test cell instrumentation.

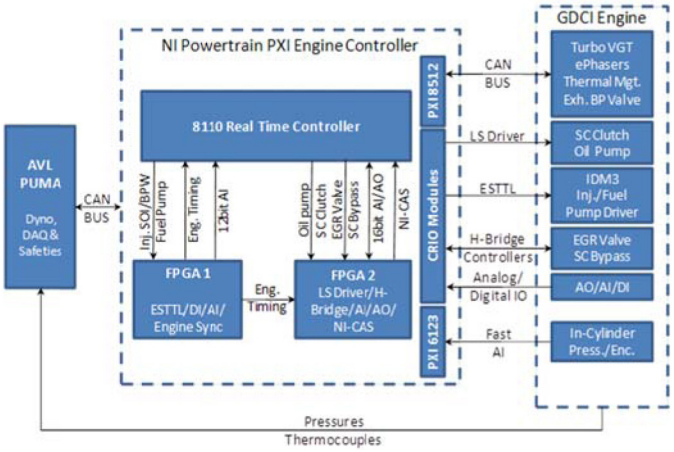


Figure 6. Schematic of Test Cell Engine Control System for GDCI Multi-cylinder Engine Testing.

Engine control software for dynamometer testing was developed by Delphi. The software balances IMEP for each cylinder based on cylinder pressure data. A multiple-injection- control utility [23] was developed to control the fuel injection quantity, Q, for each injection event. The Q for each injection is determined using instantaneous rail pressure, cylinder pressure, and an embedded calibration map for each injector. Fuel rail pressure is tightly controlled using the rail pressure sensor and the GDi fuel pump spill valve. Intake boost is controlled by the supercharger bypass valve and turbocharger rack position for minimum boost parasitics. Engine coolant temperature and liquid-cooled, charge air coolers are controlled via temperature feedback to maintain prescribed set points. The engine controller provides various other controls functions for the EGR valve, SC clutch, 2-stage oil pump, etc.

A CAN bus was used to communicate among the main controller, actuator smart controllers, and the PUMA test system in the test cell. The CAN bus passes information for site safeties, emissions, fuel flow, as well as pressure transducers and thermocouple values (Figure 6). Data acquisition of all high-speed combustion data and low-speed data is performed by the engine controller and saved in a single, binary file.

## GDCI COMBUSTION CHARACTERISTICS

In this section, the GDCI combustion process is illustrated for engine operation at 1500 rpm-6 bar IMEP using a double injection strategy. Figures 7, 8, 9, and 10 demonstrate combustion phasing control using injection parameters, while achieving low NOx, PM, and fuel consumption with good combustion stability.

Figure 7 shows the effect of the start of injection for the last injection ($SOI_{last}$) on combustion phasing (CA50). A characteristic U-shaped response is produced enabling combustion phasing to be controlled in one of two regimes. On the right side of the valley in Figure 7, $SOI_{last}$ is generally retarded. Combustion phasing retards as injection timing is retarded, similar to the response of a diesel combustion system. Ignition dwell (IDW) is relatively low. This is designated the GDCI Late Injection regime.

On the left side of the valley in Figure 7, $SOI_{last}$ is generally advanced and is designated as the GDCI Early Injection regime. For GDCI early injection, combustion phasing retards as injection timing advances. This occurs because earlier injection causes IDW to increase significantly due to lower cylinder pressure and temperature. For both GDCI late and early injection regimes, the injection process is complete prior to start of heat release, so they are considered partially premixed compression ignition (PPCI) combustion processes. The dashed lines in Figure 7 represent estimated data for these tests.

The influence of EGR for both regimes is also shown in Figure 7. The addition of EGR increases the ignition delay and retards combustion. Combustion phasing is still injection timing controlled. For the GDCI Early Injection regime, data for exhaust rebreathing is also shown. Rebreathing increases the charge temperature, which enables higher EGR or more advanced injection timing.

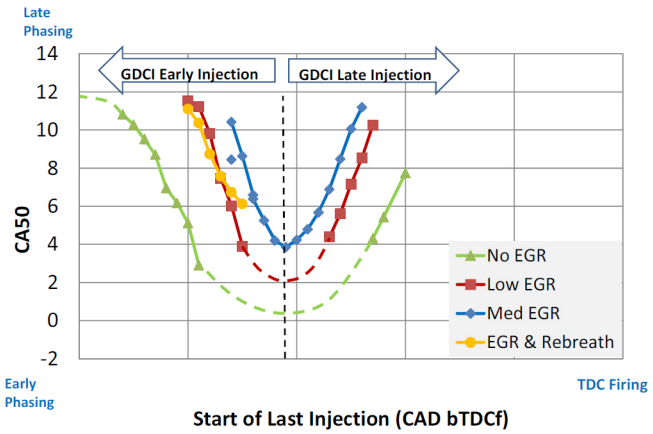


Figure 7. GDCI Combustion Phasing as a Function of Last Injection Timing, EGR, and Exhaust Rebreathing (1500 rpm-6 bar IMEP).

Figure 8 shows the influence of $SOI_{last}$, EGR and exhaust rebreathing on NOx and smoke emissions. For GDCI late injection, smoke increases as injection is retarded. The addition of EGR provides a reduction in NOx and smoke by increasing the ignition delay and the associated greater mixing. Smoke levels are reduced below the smoke target of 0.1 FSN but NOx levels still exceed the NOx target of 0.2 g/kWh in this regime.

For GDCI early injection, NOx and smoke levels are significantly reduced (Figure 8). In this regime the addition of EGR is not necessarily beneficial since the dilution effect of EGR also requires a reduction in injection timing and provides a shorter time for mixing. The net effect is a small NOx increase at constant combustion phasing. However, exhaust rebreathing provides a NOx benefit by reducing peak temperature while increasing mixing time. As shown in Figure 8, this enables a NOx reduction of approximately 50 percent at this operating condition.

Figure 9 shows ISFC as a function of $SOI_{last}$, EGR, and exhaust rebreathing. This data shows that ISFC is generally best a little on the early side of the valley. Since NOx and smoke emissions are also best in this region, this region is generally preferred for engine calibration.

Figure 10 shows combustion stability as measured by coefficient of variation of IMEP (COV IMEP). This data confirms that combustion stability in the early injection regime used for engine calibration is less than the 3% COV IMEP target.

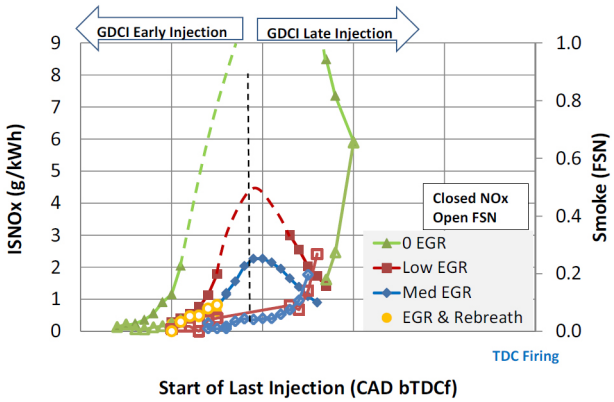


Figure 8. ISNOx and Smoke as a Function of Last Injection Timing, EGR, and Exhaust Rebreathing (1500 rpm-6 bar IMEP).

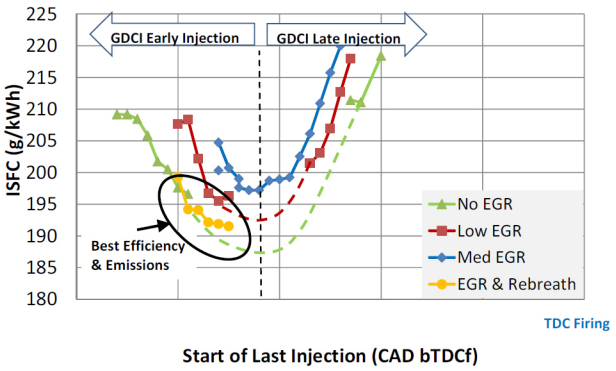


Figure 9. Indicated Specific Fuel Consumption as a Function of Injection Timing, EGR, and Exhaust Rebreathing (1500 rpm-6 bar IMEP).

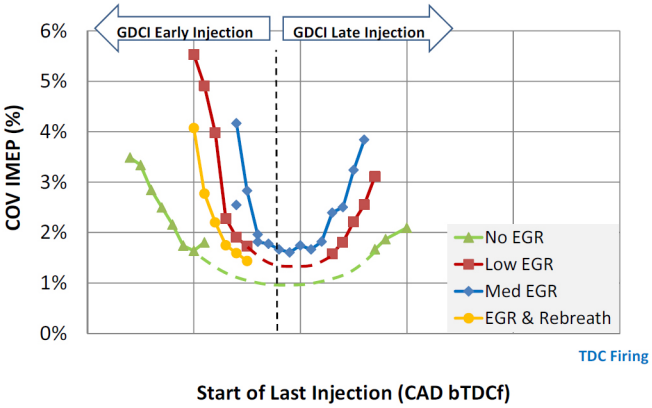


Figure 10. Combustion stability as a Function of Last Injection Timing, EGR, and Rebreathing (1500 rpm-6 bar IMEP).

## REBREATH SWEEP AT 1500 RPM-6BAR IMEP

Rebreathing hot exhaust gases raises cylinder gas temperature and promotes autoignition. Rebreathing also significantly raises exhaust gas temperature, which is essential to maintain catalyst temperatures at low loads. At low to medium loads, rebreathing enables a significant improvement in fuel consumption by reducing the MAP required for autoignition.

In this section, data is presented showing the tradeoff between MAP and rebreathing at 1500 rpm-6 bar IMEP. A revised second generation (Gen 2) exhaust manifold and catalyst system was used and is shown in Figure 11 (different from Figure 5 above). Rebreathing was increased by rotating the exhaust cam electric phaser, which increased the lift of the secondary valve event during the intake stroke.

Indicated and brake specific fuel consumption are shown in Figure 12 as rebreathing was increased and MAP was reduced from 1.6 bar to 1.2 bar. ISFC remains flat through most of the sweep and BSFC was reduced nearly 7 percent due to reduced boost parasitics. For the data presented, NOx was less than the 0.2 g/kWh target and smoke was less than 0.02 FSN (0.1 FSN target). As shown in Figure 13, COV IMEP also remained low and combustion efficiency improved for most of the MAP range.

Figure 14 shows the engine airflow and equivalence ratio during the test. As rebreathing was increased less air was inducted into the cylinder and engine airflow decreased. This increased global equivalence ratio but more importantly reduced the exhaust flow rate and space velocity through the catalyst. Figure 15 shows the very large exhaust temperature rise as rebreathing was increased. At one inch downstream of the catalyst face, temperature increased 200 degree C. When combined with lower exhaust flow rates (lower space velocities), the performance of the catalyst system was greatly improved.

The performance of the oxidation catalyst was evaluated at the 135 and 120 kPa MAP points during the rebreathe test. As shown in Figure 16, HC conversion efficiency was 97 percent and CO conversion efficiency was effectively 100 percent. NOx increased slightly during the test.

This test demonstrated that the exhaust rebreathing strategy was very effective in reducing part load boost parasitics and greatly improves catalyst performance with very low engine-out emissions and excellent combustion stability.

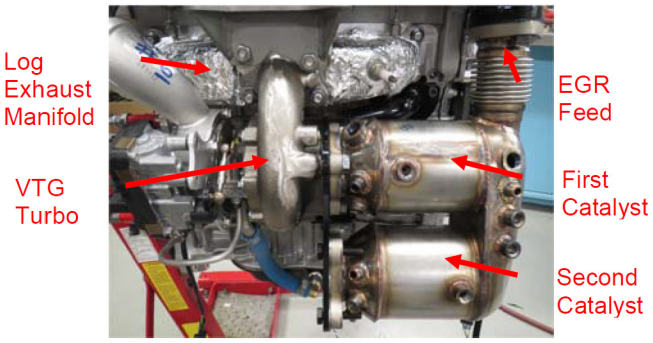


Figure 11. Gen 2 Exhaust Manifold and Oxidation Catalyst Used for Rebreathe Tests at 1500 rpm-6 bar IMEP.

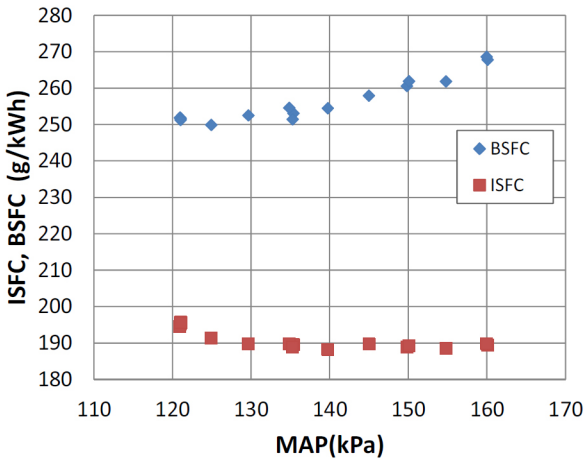


Figure 12. Improvement of Fuel Consumption Due to Increased Rebreathing and Reduced MAP at 1500 rpm-6 bar IMEP.

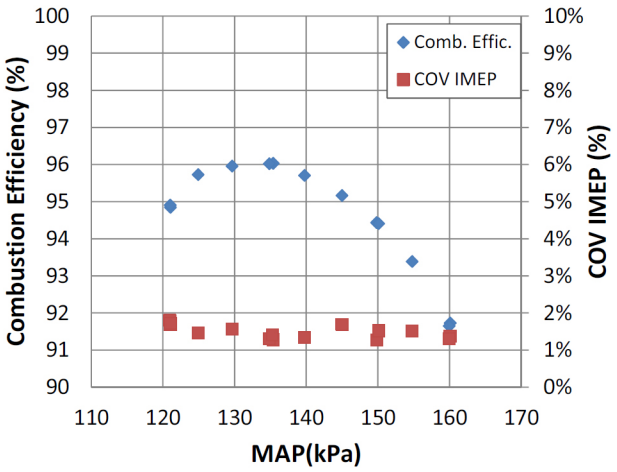


Figure 13. Combustion Stability and Efficiency as MAP and Rebreathe are Varied at 1500 rpm-6 bar IMEP.

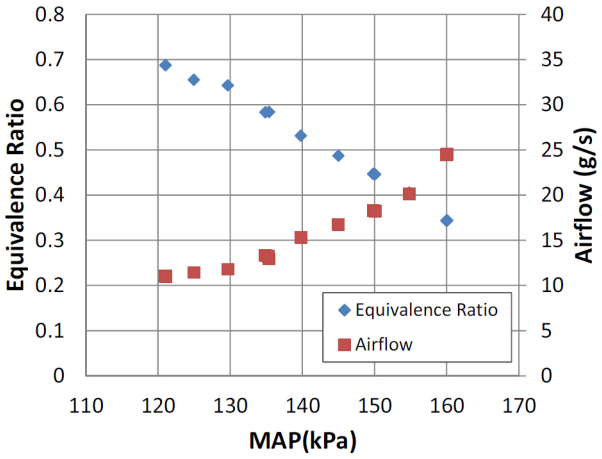


Figure 14. Reduction of Airflow and Increased Equivalence Ratio as MAP and Rebreathe are Varied at 1500 rpm-6 bar IMEP.

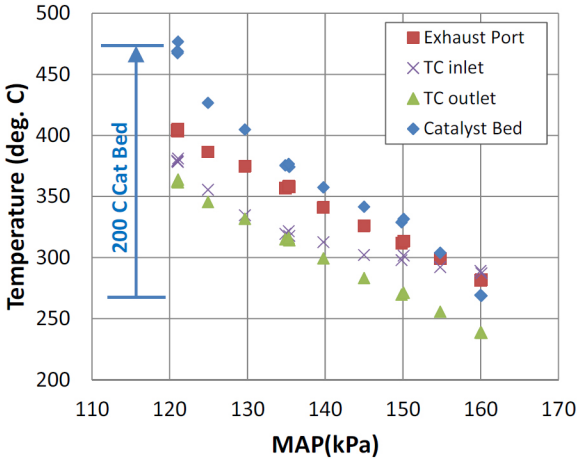


Figure 15. Exhaust System Temperatures as MAP and Rebreathe are Varied at 1500 rpm-6 bar IMEP.

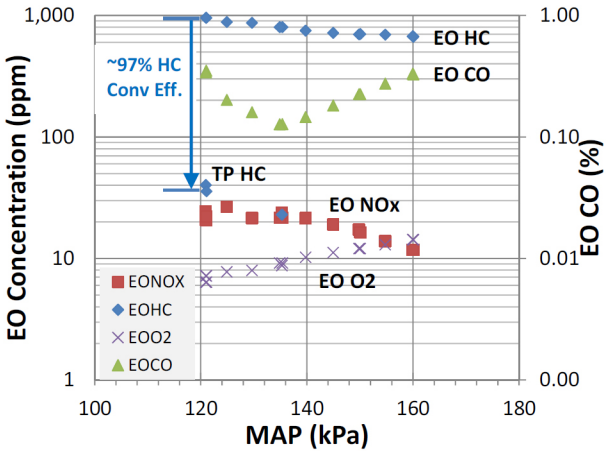


Figure 16. Engine-Out and Post-Catalyst Emissions Data for Rebreathe Tests at 1500 rpm-6 bar IMEP.

## LOAD SWEEP AT 2500 RPM

In this section, test data is presented for operation at 2500 rpm from idle to high load. For these tests, the GDCI injection system and an early injection strategy were used to produce low BSFC, NOx and smoke emissions. The data in this section is not representative of best torque or full load output.

Figure 17 shows ISFC and BSFC as a function of IMEP and BMEP, respectively. In the region under 4 bar IMEP, the engine was operated naturally aspirated with the SC bypass fully open and the turbocharger producing virtually no boost. For some test points, data is shown with and without the SC clutch engaged. Due to a reduction in parasitic loss, the declutched data shows a significant BSFC advantage and is highlighted with the outlined diamonds. Very low BSFC and ISFC are noted.

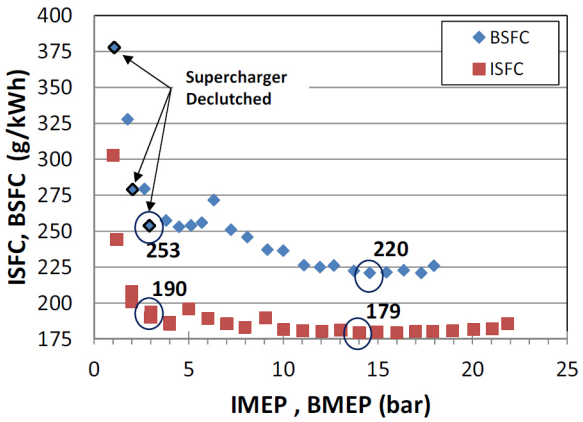


Figure 17. Fuel Consumption as a Function of Load at 2500 rpm.

To promote autoignition at low loads, an exhaust rebreathing strategy was employed. GDCI operation can be achieved without the use of rebreathing but results in reduced efficiency due to higher boost levels and associated parasitic losses.

As load was increased above 4 bar IMEP, MAP and EGR were progressively increased to maintain combustion phasing at best efficiency timing within emissions and noise constraints. CA50 and

COV IMEP are shown in Figure 18 over the load range. At higher load, injection timing control was used to retard combustion phasing to limit combustion noise. CA50 ranged from approximately 7 CAD at low load to 16 CAD at high load. COV IMEP was typically below the 3% target.

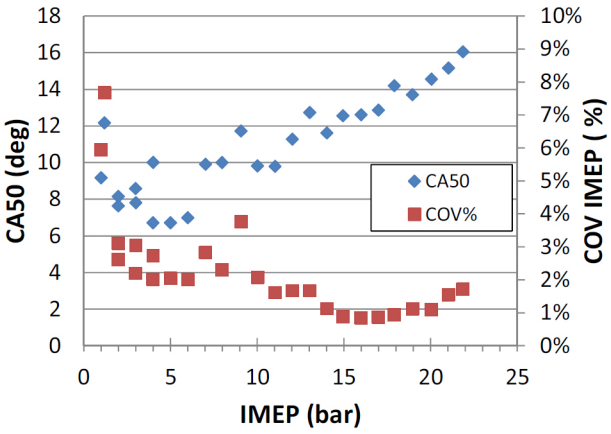


Figure 18. Combustion Phasing, CA50, and COV IMEP as a Function of IMEP at 2500 rpm.

NOx and smoke emissions are shown in Figure 19. Rebreathe, MAP, and EGR were controlled to meet a 0.2 g/kWh NOx target over the load range. However at high loads due to increasing EGR, NOx decreased significantly. Smoke was also very low over the entire load range. Decreasing NOx with load enables aggressive downspeeding and boosting without an emissions penalty and is a unique characteristic of GDCI combustion.

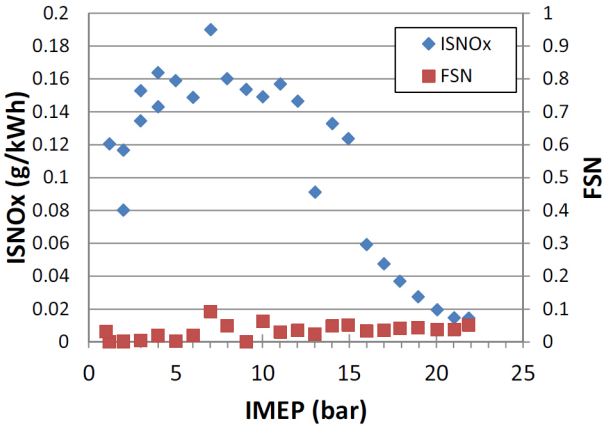


Figure 19. Indicated Specific NOx and Smoke Emissions as a Function of IMEP at 2500 rpm.

Combustion noise and 10-90 burn duration are shown in Figure 20. Combustion noise increases with load due to increased pressure rise rates and shorter burn durations. For these tests, burn duration decreased as a larger fraction of the fuel was injected in the first injection, reducing the stratification in the charge.

Peak torque for this test was reached when the global equivalence ratio equals unity. At 2500 rpm and intake air temperature of 55 deg C, maximum IMEP was 22 bar. The GDCI combustion system produced very low NOx and smoke emissions but required up to 50 percent EGR using GDCI early injection. With relaxed emissions targets and alternative injection strategies, EGR may be reduced and significantly higher output may be realized. Additional full load test data is presented in the following section.

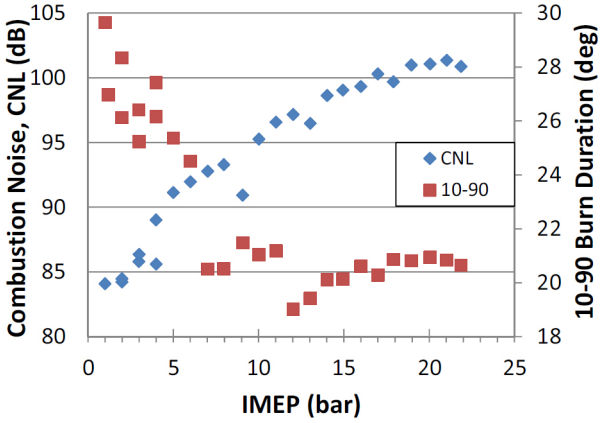


Figure 20. Combustion Noise and 10-90 Burn Duration as a Function of IMEP at 2500 rpm.

## CALIBRATION MAPPING TESTS

Engine calibration mapping tests were performed over a wide range of steady-state, warmed-up, operating conditions. The engine was equipped with the latest GDCI injection system, which represents an improvement over previously reported data [30]. The engine included all subsystems including all accessories and a complete vehicle exhaust system. Typical operating settings for these tests are listed in Table 4.

Table 4. Engine Temperatures, Air Humidity, Fuel and Lubricant Used for Calibration Mapping Tests.

| | |
|---|---|
| Coolant Temperature | 90 C |
| Oil Temperature | 90 C |
| Intake Air Temp | 55 C |
| Air Relative Humidity | 45 percent |
| Lube Oil | Mobil-1 5W-30 |
| Fuel | Shell E10 Gasoline |

For these tests, “design of experiments” methods were not used due to the high number of control factors and limited time for testing. Test results are considered preliminary and are not fully optimized.

Test results are shown in Figure 21 and 22. For all operating conditions, targets for NOx, PM, CNL, and combustion stability (COV IMEP) were fully met. Brake specific fuel consumption at all conditions was very good with indicated specific fuel consumption (ISFC) below 180 g/kWh over very wide operating ranges. Minimum BSFC of 213 g/kWh was observed at 1800 rpm-12 bar BMEP. FMEP shown in Figure 21 is significantly high for this engine. Lower BSFC is expected with improved friction characteristics in future GDCI engine developments.

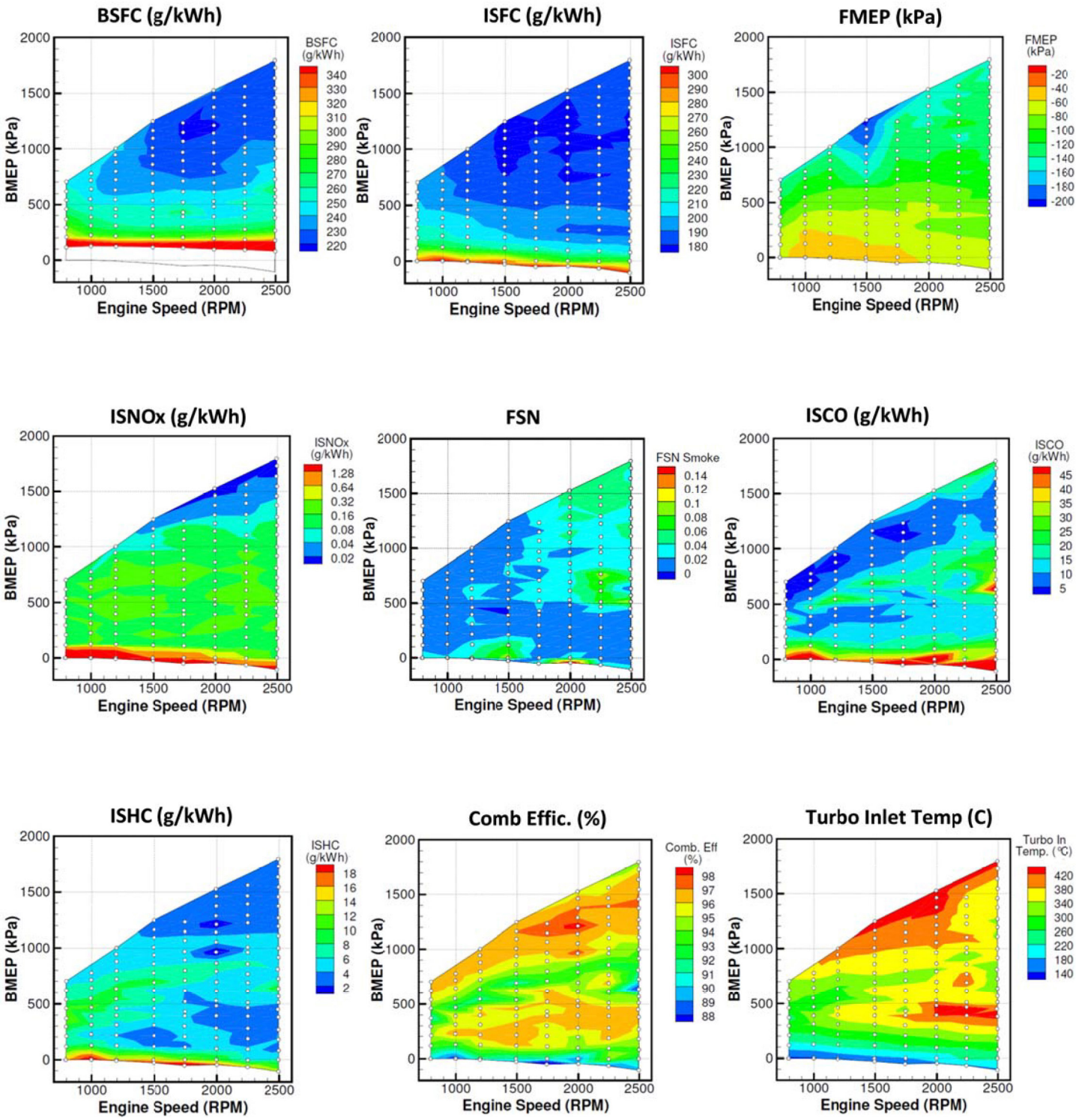


Figure 21. Measured Fuel Consumption, Emissions, and Combustion Analysis Results for Calibration Mapping Tests.

For low loads, exhaust rebreathing was very effective to promote autoignition and maintain exhaust temperatures. For the lowest loads tested, exhaust temperature at the turbocharger inlet was typically above 250 degree C. Combustion efficiency ranged from 92 to 97 percent. Further improvements in combustion efficiency are expected through the calibration and engine development processes.

For medium-to-high loads, NOx emissions exhibited a unique decreasing trend with increasing load. This is contrary to typical NOx trends for spark-ignited and diesel engines and is attributed to increasing EGR levels with load. Decreasing NOx at high load is an enabler for aggressive downspeeding and reduces NOx aftertreatment requirements.

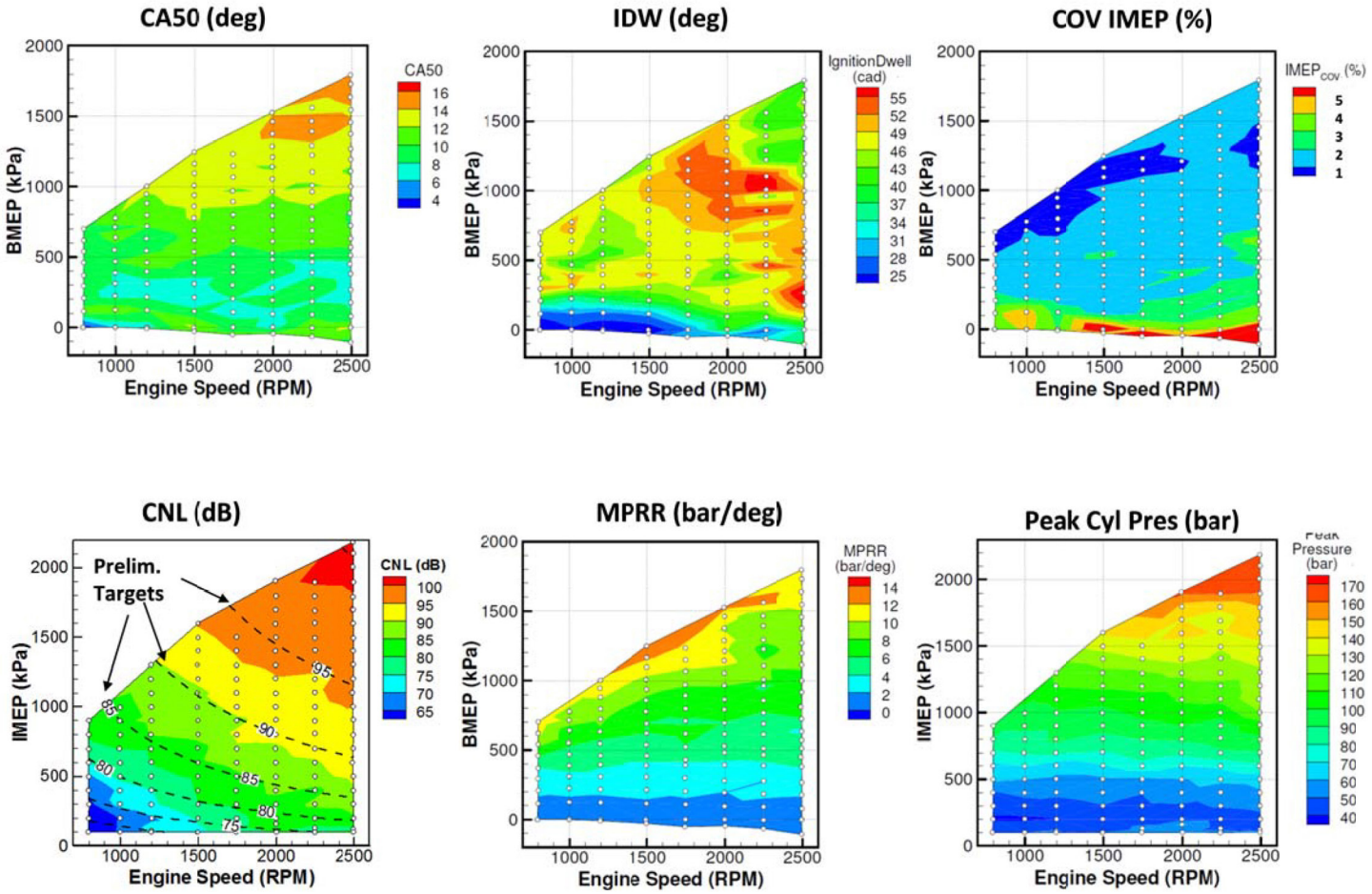


Figure 22. Measured Test Parameters and Combustion Analysis Results for Calibration Mapping Tests.

CNL data are shown in Figure 22 over the range of operating conditions. The CNL plot also shows dashed lines, which represent preliminary targets based on audible combustion noise in the dynamometer test cell. Combustion noise targets are subjective and will require validation in the vehicle for specific applications.

For all tests shown in Figure 21 and 22, peak exhaust temperatures at the turbocharger inlet were below about 500 C, which is desirable for durability of catalyst and exhaust system components. Peak cylinder pressure was less than 165 bar, inlet manifold pressure was less than 3.5 bar absolute, and EGR was less than 51 percent.

### Preliminary Full-Load Characteristics

Preliminary dynamometer tests were performed to characterize the full-load performance of the first generation GDCI multi- cylinder engine. Initial tests were conducted at 1500 rpm for intake air temperatures (IAT) of 55 and 35 degree C. Results are shown in Figures 23, 24, 25, 26, 27.

As load was increased, global equivalence ratio approached unity and injection parameters were adjusted to retard combustion phasing (CA50) to meet combustion noise targets (Figure 23). The effect of cooler IAT was significant and increased maximum output for this test by 3 bar to 19 bar IMEP.

Significant amounts of EGR were required to maintain clean combustion at higher loads. Figure 24 shows EGR and engine airflow for the test. For 55 degree C IAT, about 50 percent EGR was needed at full load. Operation at 35 degree C required significantly less EGR and increased charge density, which made more air available for higher output. In all cases, targets for NOx and FSN were met as shown in Figure 25.

NOx decreased to very low levels but exhibited higher sensitivity to EGR at full load.

Reduced intake air temperature improved ISFC somewhat as shown in Figure 26. Full load ISFC and BSFC were 177 and 238 g/kWh, respectively. Combustion stability was very good at approximately 1 percent COV IMEP.

As expected, “mean” peak cylinder pressure (PCP) and combustion noise (CNL) increased as load increased (Figure 27). At full load for this test, PCP was 160 bar and safely below rated cylinder pressure of 200 bar. CNL was approximately 95 dB, which was also below noise targets for this speed.

Preliminary full load tests were also conducted for engine speeds from 1500 to 3000 rpm using alternative injection and control strategies. For these tests, the objective was to produce high torque rather than minimum BSFC and emissions as for calibration mapping tests. For these tests, intake air temperature of 40 degree C, maximum EGR of 40 percent, and maximum MAP of 3.5 bar were used. Results for these preliminary tests are shown in Figure 28. The data is limited to the speed range shown and does not indicate the potential torque curve for higher speed operation.

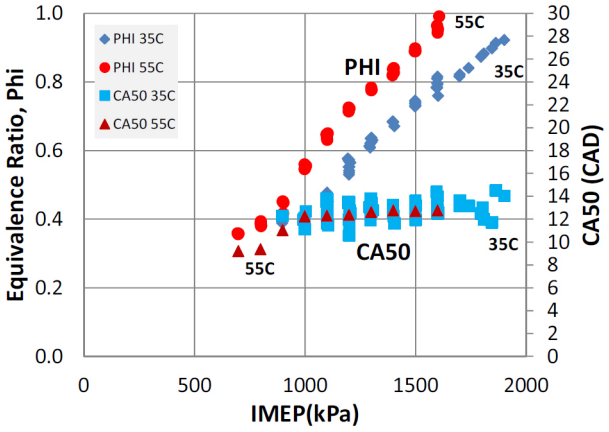


Figure 23. Equivalence Ratio and CA50 as a Function of IMEP at 1500 rpm for 35C and 55C Intake Air Temperature.

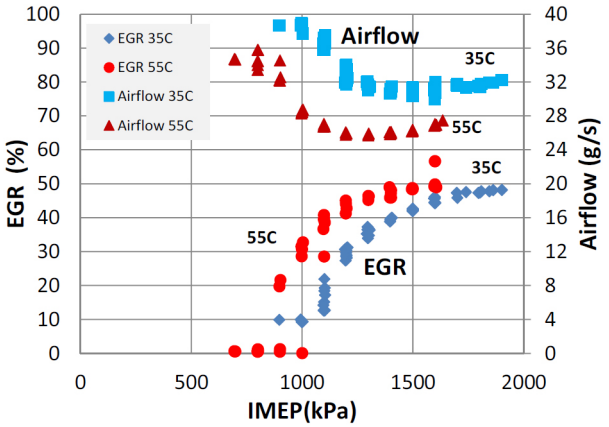


Figure 24. EGR and Engine Airflow as a Function of IMEP at 1500 rpm for 35C and 55C Intake Air Temperature.

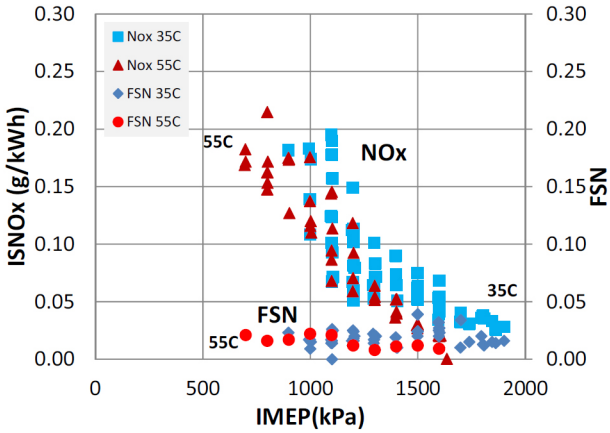


Figure 25. NOx and Smoke (FSN) Emissions as a Function of IMEP at 1500 rpm for 35C and 55C Intake Air Temperature.

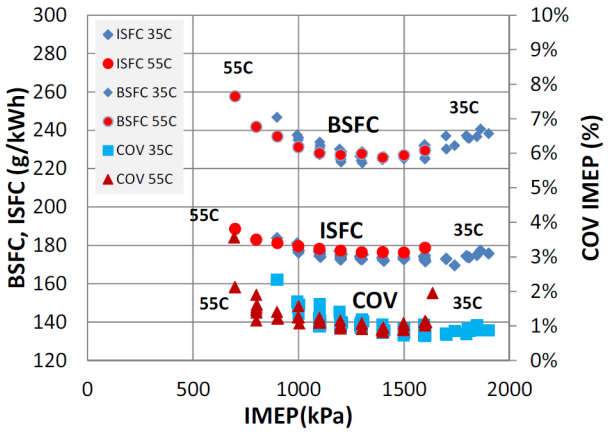


Figure 26. BSFC, ISFC, and COV IMEP as a Function of IMEP at 1500 rpm for 35C and 55C Intake Air Temperature.

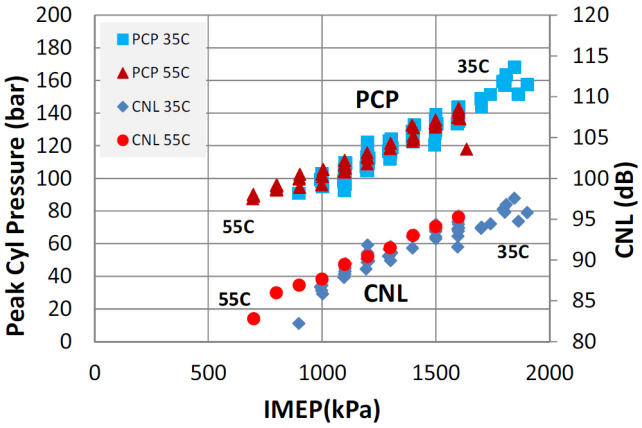


Figure 27. Peak Cyl. Pressure and Combustion Noise as a Function of IMEP at 1500 rpm for 35C and 55C Intake Air Temperature.

The data shows that good low-speed and medium-speed torque can be achieved using the GDCI combustion system. By reducing intake air temperature and reducing EGR, more air was available and fuelling levels could be increased. At 1500, 2000, and 2500 rpm, the engine was operated near stoichiometry, and the resulting torque was representative of GDCI combustion using this injection strategy. However, at 3000 rpm, global equivalence ratio was only 0.85. This indicates that considerable excess air was still available and higher BMEP may be achieved at higher fuelling levels.

For all the tests in Figure 28, engine out NOx emissions were very low and below the program target of 0.2 g/kWh. Exhaust gas temperatures were also very low and did not exceed 600 C for these tests. “Mean” peak cylinder pressure was less than 200 bar, which was the PCP rating for this engine. Overall, while additional full load development is needed, these results meet expectations for the first generation GDCI multi-cylinder engine. With over 1550 accumulated test hours, base engine durability (cylinder head, valvetrain, piston-rings, bearings) appears very good.

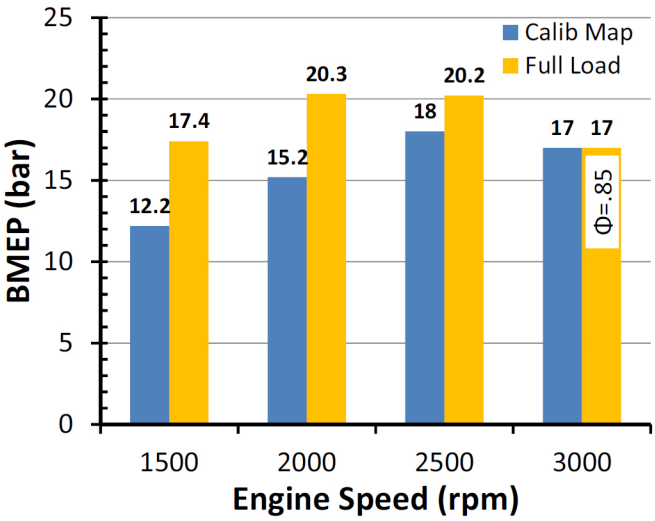


Figure 28. Full load BMEP Compared to BMEP for Calibration Mapping for Engine Speeds up to 3000 rpm.

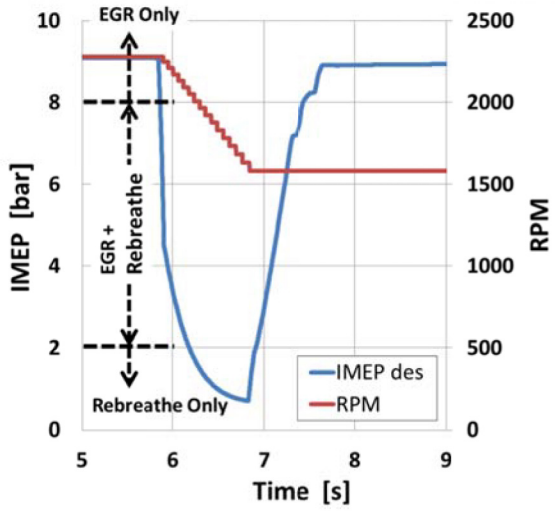


Figure 29. Desired Engine IMEP and Speed During a Gear Shift.

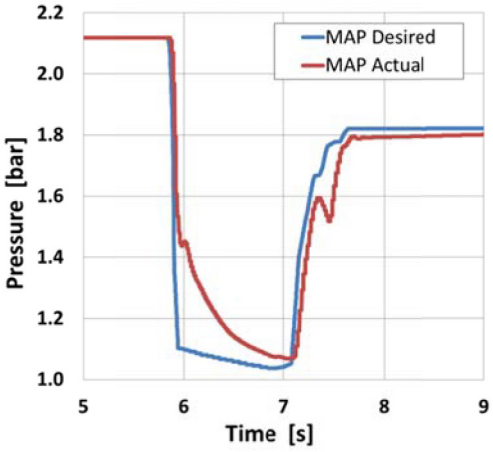


Figure 30. Desired and Actual MAP During a Gear Shift.

## TRANSIENT CO-SIMULATION FOR GEAR SHIFT

Co-simulation using Matlab Simulink [35] and GT-Suite [37] has been applied extensively to investigate engine system design and control issues, such as thermal management, cold start and warm up, intake air temperature control, boost control, and EGR control. This section presents simulation studies that address the problem of engine control during a fast gear shift with a manual transmission. The challenge is to maintain stable combustion with proper combustion phasing and acceptable combustion noise. A test vehicle for the project was equipped with a manual transmission and represents the worst case for gear shift transients (i.e., as opposed to automatic transmissions).

Figure 29 shows desired engine IMEP and engine speed for a typical upshift logged during a vehicle FTP city test. Note the high rate of decrease in desired IMEP (approximately100 bar/s) early in the tip-out phase. This is needed to avoid a speed flare to achieve a smooth shift. After clutch re-engagement, it is followed by a tip-in having an IMEP rise rate of 15 bar/s. Desired and actual MAP also fall and rise rapidly as shown in Figure 30.

During a gearshift tip-out the engine must transition rapidly between three zones of operation, as indicated in Figure 29. Initially at high load there is EGR and little or no exhaust rebreathing. As IMEP and engine speed decrease, MAP decreases and less EGR is required. Increased rebreathing is required in order to maintain auto-ignition temperatures. At the lowest IMEP, EGR is turned off and significant rebreathing is required. Fast control of this process is difficult because: a) turbo lag holds MAP higher than desired, as shown in Figure 30, b) the low-pressure EGR system, due to its large volume, has significant transport and mixing delay, and c) to increase rebreathing, secondary exhaust valve lift must be applied rapidly, while exhaust pressure must be controlled above intake pressure. Engine delta-P is defined as exhaust pressure minus intake pressure, and is required to drive rebreathe flows.

Measured IMEP from cylinder pressure data and desired IMEP during the transient are shown in Figure 31. Misfires and partial burns may occur early in the tip-out event, and persist until the tip-in event. Figures 32, 33, and 34 show the reasons for this behavior. Engine delta-P does not achieve positive values until well into the tip-out event. Consequently as shown in Figure 33, rebreathe flow develops slowly and compression temperature rises slowly (Figure 34). In addition, EGR, which demotes auto-ignition, persists due to the inherent delay associated with low-pressure EGR systems (Figure 33).

The data in Figure 31 shows that to avoid misfires a large amount of rebreathe must develop within 150 ms from start of tip-out. Several methods have been investigated to improve rebreathe response, including improved VTG rack and boost control.

The effectiveness of these steps was evaluated using co- simulation. Figures 35, 36, and 37 show the improvement in delta-P, rebreathe and cylinder temperature responses relative to the baseline case, respectively. The combined effect on compression temperature at 150 ms after start of tip-out, when misfire begins for the baseline case, was 91 K. At 250 ms, compression temperature was 185 K higher.

This represents a significant improvement in transient rebreathe response of the system and should enable robust gearshifts over a range of transient operating conditions.

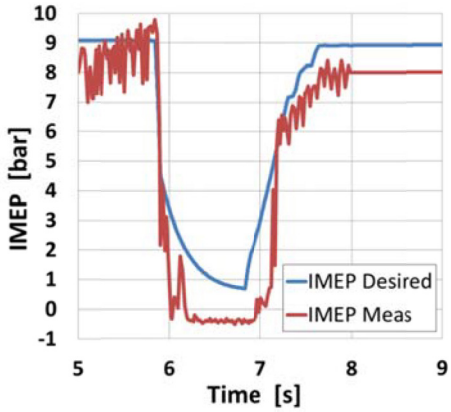


Figure 31. Measured and Desired IMEP During Vehicle Test.

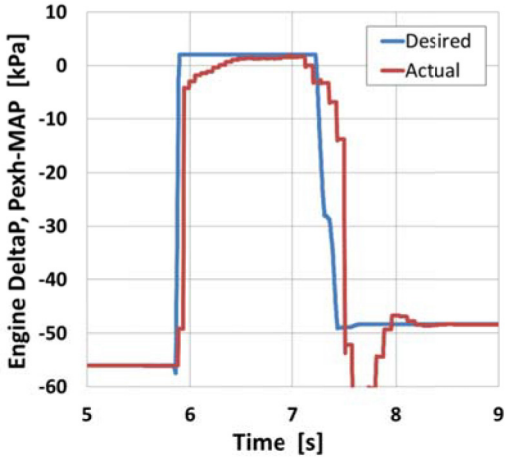


Figure 32. Engine Delta-P Response During a Gear Shift.

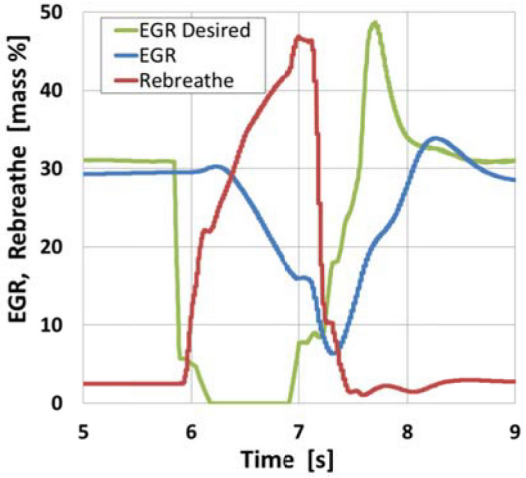


Figure 33. EGR and Rebreathe Response During a Gear Shift.

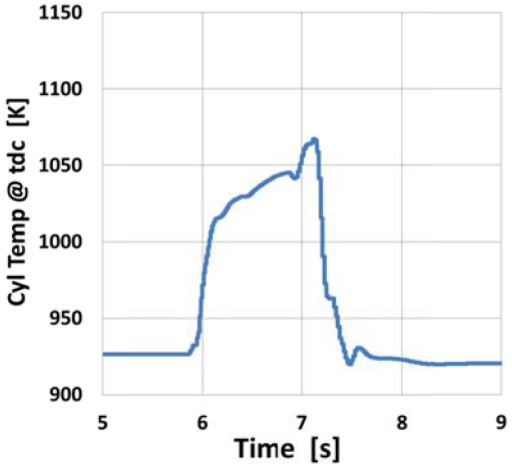


Figure 34. Cylinder Unburned Gas Temperature at TDC.

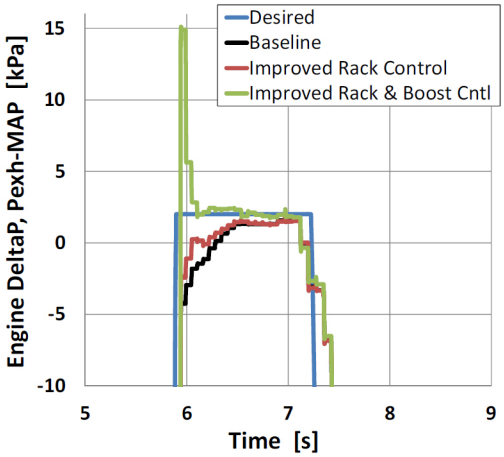


Figure 35. Engine Delta-P Response for Steps 1 and 2.

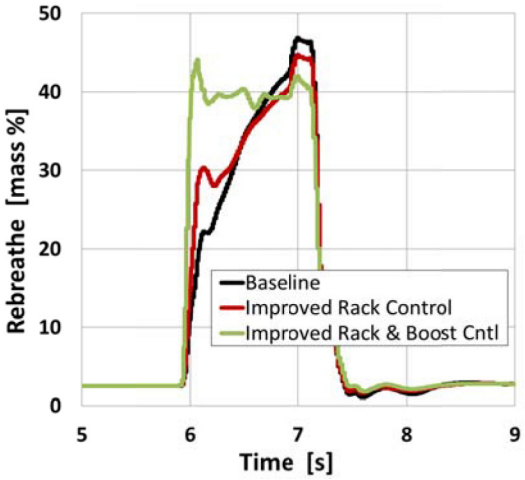


Figure 36. Rebreathe Response for Steps 1 and 2.

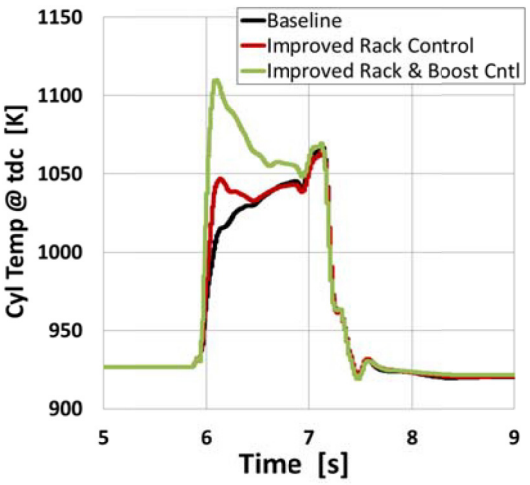


Figure 37. Compression Temperature Response for Steps 1 and 2.

## SUMMARY

Building on previous developments and extensive simulation work, a 1.8L four-cylinder GDCI engine was developed and tested using market gasoline (RON91) at Delphi. The engine uses a new low-temperature combustion process for gasoline partially-premixed compression ignition. Central to these advancements was a fuel injection system and injection strategy combined with a new piston design. Using multiple late injections and GDi-like fuel pressure, the fuel-air mixture could be stratified but sufficiently mixed. This produced robust ignition with very clean, efficient, and stable combustion within constraints for combustion noise.

Part load test data showed the fundamental characteristics of GDCI combustion and differentiated GDCI early injection from GDCI late injection.

Part load tests were performed that showed rebreathing hot exhaust gases was very effective to reduce boost parasitics and greatly improve catalyst performance. Very low emissions and excellent combustion stability were demonstrated during the test.

Extensive steady-state, calibration tests were performed with the latest GDCI injection system. Test results showed that targets for NOx (0.2 g/kWh), smoke (0.1 FSN), combustion noise, and stability (3% COV IMEP) were met. Injection parameters could be used at all operating conditions to control combustion phasing. At all conditions, GDCI was remarkably clean with the potential for no or reduced aftertreatment for NOx and particulate emissions. Further BSFC improvements are expected through planned development work.

Preliminary full-load tests were performed. At 1500 rpm, reduced intake air temperature improved full load output by 3 bar IMEP. Additional preliminary full load tests at 1500 to 3000 rpm were reported for reduced intake air temperature (40 C) and reduced EGR (40 percent). While very good low-speed and medium-speed BMEP was reported, more work is needed to develop output characteristics of the engine.

Transient co-simulations were performed for an aggressive gear shift using a manual transmission. The dynamics of the process were explored and methods to improve combustion control during the gear shift were shown. The fast responses of the exhaust rebreathe system and the boost system enabled robust combustion control for an aggressive gear shift transient.

## REFERENCES


1. Kalghatgi, G., “Auto-Ignition Quality of Practical Fuels and Implications for Fuel Requirements of Future SI and HCCI Engines,” SAE Technical Paper 2005-01-0239, 2005, doi:10.4271/2005-01-0239.
2. Johansson, B., “High-Load Partially Premixed Combustion in a Heavy-Duty Diesel Engine, Diesel Engine Emissions Reduction (DEER) Conference Presentations, 2005, Chicago, IL.
3. Risberg, P., Kalghatgi, G., Ångstrom, H., and Wåhlin, F., “Auto-ignition quality of Diesel-like fuels in HCCI engines,” SAE Technical Paper 2005-01-2127, 2005, doi:10.4271/2005-01-2127.
4. Kalghatgi, G., Risberg, P., and Ångström, H., “Advantages of Fuels with High Resistance to Auto-ignition in Late-injection, Low-temperature, Compression Ignition Combustion,” SAE Technical Paper 2006-01-3385, 2006, doi:10.4271/2006-01-3385.
5. Kalghatgi, G., Risberg, P., and Ångström, H., “Partially Pre-Mixed Auto-Ignition of Gasoline to Attain Low Smoke and Low NOx at High Load in a Compression Ignition Engine and Comparison with a Diesel Fuel,” SAE Technical Paper 2007-01-0006, 2007, doi:10.4271/2007-01-0006.
6. Kalghatgi, G., “Low NOx and Low Smoke Operation of a Diesel Engine using Gasoline-Like Fuels”, ASME 2009 International Combustion Engine Division Spring Technical Conference, ICES2009-76034, 2009.
7. Manente, V., Johansson, B., and Tunestal, P., “Partially Premixed Combustion at High Load using Gasoline and Ethanol, a Comparison with Diesel,” SAE Technical Paper 2009-01-0944, 2009, doi:10.4271/2009-01-0944.
8. Manente, V., Johansson, B., and Tunestal, P., “Half Load Partially Premixed Combustion, PPC, with High Octane Number Fuels. Gasoline and Ethanol Compared with Diesel”, SIAT 2009 295, 2009.
9. Manente, V., Johansson, B., and Tunestal, P., “Characterization of Partially Premixed Combustion with Ethanol: EGR Sweeps, Low and Maximum Loads”, ASME International Combustion Engine Division 2009 Technical Conference, ICES2009-76165, 2009.
10. Manente, V., Tunestal, P., Johansson, B., and Cannella, W., “Effects of Ethanol and Different Type of Gasoline Fuels on Partially Premixed Combustion from Low to High Load,” SAE Technical Paper 2010-01-0871, 2010, doi:10.4271/2010-01-0871.
11. Weall, A. and Collings, N., “Gasoline Fuelled Partially Premixed Compression Ignition in a Light Duty Multi Cylinder Engine: A Study of Low Load and Low Speed Operation,” *SAE Int. J. Engines* 2(1):1574-1586, 2009, doi:10.4271/2009-01-1791.
12. Ra, Y., Yun, J.E., and Reitz, R., “Numerical Simulation of Diesel and Gasoline-fueled Compression Ignition Combustion with High-Pressure Late Direct Injection,” Int. J. Vehicle Design, Vol. 50, Nos. 1,2,3,4. pp.3-34, 2009.
13. Ra, Y., Yun, J.E., and Reitz, R., “Numerical Parametric Study of Diesel Engine Operation with Gasoline,” Comb. Sci. and Tech., 181:350-378, 2009.
14. Dempsey, A. and Reitz, R., “Computational Optimization of a Heavy-Duty Compression Ignition Engine Fueled with Conventional Gasoline,” *SAE Int. J. Engines* 4(1):338-359, 2011, doi:10.4271/2011-01-0356.
15. Ra, Y., Loeper, P., Reitz, R., Andrie, M. et al., “Study of High Speed Gasoline Direct Injection Compression Ignition (GDICI) Engine Operation in the LTC Regime,” *SAE Int. J. Engines* 4(1):1412-1430, 2011, doi:10.4271/2011-01-1182.
16. Ra, Y., Loeper, P., Andrie, M., Krieger, R. et al., “Gasoline DICI Engine Operation in the LTC Regime Using Triple-Pulse Injection,” *SAE Int. J. Engines* 5(3):1109-1132, 2012, doi:10.4271/2012-01-1131.
17. Ciatti, S., and Subramanian, S., “An Experimental Investigation of Low Octane Gasoline in Diesel Engines,” ASME International Combustion Engine Division 2010 Technical Conference, ICEF2010-35056, 2010.
18. Das Adhikary, B., Ra, Y., Reitz, R., and Ciatti, S., “Numerical Optimization of a Light-Duty Compression Ignition Engine Fuelled With Low-Octane Gasoline,” SAE Technical Paper 2012-01-1336, 2012, doi:10.4271/2012-01-1336.

19. Ciatti, S., Johnson, M., Das Adhikary, B., Reitz, R. et al., "Efficiency and Emissions performance of Multizone Stratified Compression Ignition Using Different Octane Fuels," SAE Technical Paper 2013-01-0263, 2013, doi:10.4271/2013-01-0263.
20. Das Adhikary, B., Reitz, R., and Ciatti, S., "Study of In-Cylinder Combustion and Multi-Cylinder Light Duty Compression Ignition Engine Performance Using Different RON Fuels at Light Load Conditions," SAE Technical Paper 2013-01-0900, 2013, doi:10.4271/2013-01-0900.
21. Yang, H., Shuai, S., Wang, Z., and Wang, J., "High Efficiency and Low Pollutants Combustion: Gasoline Multiple Premixed Compression Ignition (MPCI)," SAE Technical Paper 2012-01-0382, 2012, doi:10.4271/2012-01-0382.
22. Won, H., Peters, N., Pitsch, H., Tait, N. et al., "Partially Premixed Combustion of Gasoline Type Fuels Using Larger Size Nozzle and Higher Compression Ratio in a Diesel Engine," SAE Technical Paper 2013-01-2539, 2013, doi:10.4271/2013-01-2539.
23. Sellnau, M., Sinnamon, J., Hoyer, K., and Husted, H., "Gasoline Direct Injection Compression Ignition (GDCI) - Diesel-like Efficiency with Low CO2 Emissions," *SAE Int. J. Engines* 4(1):2010-2022, 2011, doi:10.4271/2011-01-1386.
24. Sellnau, M., Sinnamon, J., Hoyer, K., and Husted, H., "Development of Full-Time Gasoline Direct-Injection Compression Ignition (GDCI) for High Efficiency and Low CO2, NOx and PM," Aachen Colloquium 2011, 2011.
25. Sellnau, M., Sinnamon, J., Hoyer, K., and Husted, H., "Full-Time Gasoline Direct-Injection Compression Ignition (GDCI) for High Efficiency and Low NOx and PM," *SAE Int. J. Engines* 5(2):300-314, 2012, doi:10.4271/2012-01-0384.
26. Hoyer, K., Sellnau, M., Sinnamon, J., and Husted, H., "Boost System Development for Gasoline Direct-Injection Compression-Ignition (GDCI)," *SAE Int. J. Engines* 6(2):815-826, 2013, doi:10.4271/2013-01-0928.
27. Sellnau, M., Sinnamon, J., Hoyer, K., Kim, J. et al., "Part-Load Operation of Gasoline Direct-Injection Compression Ignition (GDCI) Engine," SAE Technical Paper 2013-01-0272, 2013, doi:10.4271/2013-01-0272.
28. Chang, J., Kalghatgi, G., Amer, A., Adomeit, P. et al., "Vehicle Demonstration of Naphtha Fuel Achieving Both High Efficiency and Drivability with EURO6 Engine-Out NOx Emission," *SAE Int. J. Engines* 6(1):101-119, 2013, doi:10.4271/2013-01-0267.
29. Chang, J., Viollet, Y., Amer, A., and Kalghatgi, G., "Fuel Economy Potential of Partially Premixed Compression Ignition (PPCI) Combustion with Naphtha Fuel," SAE Technical Paper 2013-01-2701, 2013, doi:10.4271/2013-01-2701.
30. Sellnau, M., Foster, M., Hoyer, K., Moore, W. et al., "Development of a Gasoline Direct Injection Compression Ignition (GDCI) Engine," *SAE Int. J. Engines* 7(2):2014, doi:10.4271/2014-01-1300.
31. MODEL 379020 ROTATING DISK THERMODILUTER, Operation Manual, TSI Incorporated, June, 2009.
32. MODEL 3090 ENGINE EXHAUST PARTICLE SIZE SPECTROMETER, Operation Manual, TSI Incorporated, October, 2010.
33. AVL List, "Product Description - FlexIFEM Indi," http://www.avl.com/c/document_library, Mar. 2013.
34. Labview RT Software, Release 2012, National Instruments, Austin TX, 2012.
35. Matlab Simulink Software, Mathworks, Inc., Natick, MA, 2014.
36. GT Power Software, Version 7, Gamma Technologies, Inc., Westmont, IL, 2014.


## CONTACT INFORMATION


Mark Sellnau
Engineering Manager
Delphi Advanced Powertrain
3000 University Drive
Auburn Hills, MI 48326
mark.sellnau@delphi.com


## ACKNOWLEDGMENTS


This work was supported by the US Department of Energy, Office of Vehicle Technology, and administered by Gurpreet Singh under contract DOE DE-EE0003258.

The authors gratefully acknowledge collaboration with and support from Hyundai Motor Company. The authors also appreciate contributions to this work from engineers and technicians at Delphi Powertrain, Delphi Diesel Systems; Delphi Thermal Systems, Delphi Electronics and Safety, and Delphi Korean Automotive Components.


## DEFINITIONS/ABBREVIATIONS

**atdc** - After Top Dead Center

**B** - Bore

**BDC** - Bottom Dead Center

**BMEP** - Brake Mean Effective Pressure

**BSFC** - Brake Specific Fuel Consumption

**C** - Centigrade

**CAC** - Charge Air Cooler

**CAN** - Controller Area Network

**CE** - Combustion efficiency

**CFD** - Computational Fluid Dynamics

**CNL** - Combustion Noise Level

**CO** - Carbon monoxide emissions

**COV IMEP** - Coefficient of Variation of IMEP

**DoE** - Design of Experiments

**E00** - Gasoline without Ethanol

**E10** - Gasoline with 10% Ethanol

**EEPS** - Eng. Exh Particle Size Spectra

**EGR** - Exhaust gas recirculation

**FIE** - Fuel injection equipment

**FSN** - Filtered Smoke Number

**GCR** - Geometric Compression Ratio

**GDi** - Gasoline Direct Injection

**GDCI** - Gasoline Direct Inj. Comp. Ignition

**HC** - Hydrocarbon emissions

**HCCI** - Homo. Charge Comp. Ignition

**HRR** - Heat Release Rate

**IAT** - Intake Air Temperature

**IMEP** - Indicated Mean Effective Pressure

**ISCO** - Indicated specific carbon monoxide

**ISFC** - Indicated specific fuel consumption

**ISHC** - Indicated specific hydrocarbon

**ISNOx** - Indicated specific nitrous oxide

**KIVA** - Comput. Fluid Dyn. Code developed at Los Alamos National Labs

**l** - Connecting Rod Length

**LTC** - Low Temperature Combustion

**LHV** - Lower Heating Value

**MAP** - Manifold Absolute Pressure

**M-FMEP** - Motoring Friction Mean Eff. Pres.

**MLI** - Multiple Late Injection

**NMEP** - Net Mean Effective Pressure

**NOx** - Oxides of Nitrogen

**PCP** - Peak Cylinder Pressure

**PHI** - Equivalence Ratio

**PID** - Proport., Integ., Deriv. Controller

**Pinj** - Injection Pressure

**PM** - Particulate Matter

**PPCI** - Partially Premixed Comp. Ignition

**Q** - Quantity injected

**r** - Crank throw length

**RB** - Rebreath

**RON** - Research Octane Number

**S** - Stroke

**SGDI** - Stratified Gasoline Direct Injection

**SOC** - Start of Combustion

**SOI** - Start of Injection

**SC** - Supercharging

**TC** - Turbocharging

**TDC** - Top dead center